Self-Aligning Mechanism Improves Comfort and Performance With a Powered Knee Exoskeleton

Sergei V. Sarkisian, Marshall K. Ishmael, and Tommaso Lenzi, *Member, IEEE*

***Abstract*— Misalignments between powered exoskeleton joints and the user's anatomical joints are inevitable due to difficulty locating the anatomical joint axis, non-constant location of the anatomical joint axis, and soft-tissue deformations. Self-aligning mechanisms have been proposed to prevent spurious forces and torques on the user's limb due to misalignments. Several exoskeletons have been developed with self-aligning mechanisms based on theoretical models. However, there is no experimental evidence demonstrating the efficacy of self-aligning mechanisms in lower-limb exoskeletons. Here we show that a lightweight and compact self-aligning mechanism improves the user's comfort and performance while using a powered knee exoskeleton. Experiments were conducted with 14 able-bodied subjects with the self-aligning mechanism locked and unlocked. Our results demonstrate up to 15.3% increased comfort and 38% improved performance when the self-aligning mechanism was unlocked. Not surprisingly, the spurious forces and torques were reduced by up to 97% when the self-aligning mechanism was unlocked. This study demonstrates the efficacy of self-aligning mechanisms in improving comfort and performance for sit-to-stand and position tracking tasks with a powered knee exoskeleton.**

***Index Terms*— Human-robot misalignment, exoskeleton comfort, rehabilitation robotics, wearable robotics.**

I. Introduction

POWERED exoskeletons have been proposed for rehabilitation [1], assistance [2]–[5], strength amplification [6], and productivity enhancement [7]. Regardless of the specific application, powered exoskeletons must physically interact with the wearer in a way that is comfortable and effective. Accomplishing these goals in a powered exoskeleton is challenging due to both the inter-subject and intra-subject variability of human anatomy. As the global powered exoskeleton market grows, it is important to understand how the physical human-robot interface (pHRI) affects the user's comfort and performance.

In the design of powered exoskeletons, anatomical knee joints are frequently modeled as simple pin joints. However, anatomical knee joints have a non-constant, moving axis of rotation, resulting in rotational and translational movements [8]. Even if these complex, multi-axis rotational/translational movements are disregarded, a perfect alignment of the anatomical and the exoskeleton joints is not possible because the anatomical axis cannot be perfectly located visually or by palpation. In addition, even if an exoskeleton has been aligned with the anatomical joint, it can become misaligned because of the deformation of soft tissues resulting from physical interaction with the robot [9]. Similarly, the flexibility of the physical human-robot interface may produce misalignments when transmitting forces and torques to the user. No matter the source, misalignments can lead to spurious forces and torques on the user [10]. These spurious forces and torques may load the joint and produce stress on the user's skin, potentially reducing comfort and deteriorating performance.

To address the issue of misalignment, researchers have proposed adding self-aligning mechanisms (SAM) to powered exoskeletons. Theoretical models predict that self-aligning mechanisms can reduce the spurious forces and torques on the user's limb [11]–[13]. Based on these theoretical models, numerous powered exoskeletons have been designed with self-aligning mechanisms for both the lower-limb [1], [5], [14]–[20] and the upper limb [21], [22], [12], [23]–[25]. However, no previous study has ever tested the effects of the self-aligning mechanism on the user's comfort and performance when using a lower-limb exoskeleton. Thus, there is no experimental evidence supporting the efficacy of self-aligning mechanisms.

In this paper, we investigate, for the first time, the effects of a self-aligning mechanism on the user's comfort and performance with a powered knee exoskeleton. Theoretical models are essential to design self-aligning mechanisms that effectively avoid spurious forces and torques on the user's limb [13]. However, experiments are necessary to validate these theoretical models. Theoretical models assume that self-aligning mechanisms are massless, frictionless, and infinitely stiff. These assumptions are not satisfied in physical systems. The mass of the mechanism introduces unmodeled forces and torques due to inertia and gravity, which can impair the function of the self-aligning mechanism. Unmodeled friction can prevent the passive joints of the self-aligning mechanism from moving freely under load, which is necessary for dynamic alignment. Flexion of the self-aligning mechanism's linkages introduces unmodeled movements of the passive joints so that

Manuscript received August 5, 2020; revised January 25, 2021 and March 3, 2021; accepted March 4, 2021. Date of publication March 8, 2021; date of current version March 12, 2021. This work was supported in part by the National Institute for Occupational Safety and Health under Grant T42/CCT810426 and in part by the US Department of Defense under Grant W81XWH-16-1-0701. *(Corresponding author: Sergei V. Sarkisian.)*

The authors are with the Department of Mechanical Engineering, Utah Robotics Center, The University of Utah, Salt Lake City 84112 USA (e-mail: sergei.sarkisian@utah.edu).

Digital Object Identifier 10.1109/TNSRE.2021.3064463

TABLE I
PREVIOUS STUDIES ON EXOSKELETONS AND HUMAN-ROBOT MISALIGNMENT

Study	Exo actuation type	Self-aligning?	Assisted joints	pDOFs movement measured?	Interaction forces measured?	Locked/ unlocked tested?	Subject Number	Comfort rated?	NASA TLX rated?
Lower-Limb Exoskeletons									
This study	**Powered**	**Yes**	**Knee**	**No**	**Yes**	**Yes**	**14 AB**	**Yes**	**Yes**
Sarkisian *et al., TMRB* [9]	Powered	Yes	Knee	Yes	Yes	No	4 AB	No	No
Ergin *et al., IROS* [1]	Powered	Yes	Knee	No	No	No	–	No	No
Saccares *et al., IROS* [5]	Powered	Yes	Knee	No	Yes	No	–	No	No
Lee *et al., TMECH* [38]	Powered	Yes	Hip,knee,ankle	No	Yes	No	1 AB	No	No
Junius *et al., TBME* [39]	Passive	Yes	Hip	No	No	No	4 AB	No	No
Beil *et al., ICORR* [40]	Powered	Yes	Hip	No	No	No	–	No	No
Wang *et al., RAL* [41]	Powered	Yes	Knee	Yes	No	No	–	No	No
Giovacchini *et al., RAS* [19]	Powered	Yes	Hip	No	No	No	1 AB	No	No
Choi *et al., EMBC* [42]	Powered	Yes	Knee	Yes	No	No	–	No	No
Kim *et al., IJARS* [16]	Powered	Yes	Knee	No	No	No	1 AB	No	No
Celebi *et al., IROS* [15]	Powered	Yes	Knee	Yes	No	No	1 AB	No	No
Niu *et al., Mech-Sci* [43]	Powered	Yes	Knee	Yes	Yes	No	1 AB	No	No
Cai *et al., EMBC* [14]	Powered	Yes	Knee	No	Yes	No	1 AB	No	No
Niu *et al., ReMAR* [44]	Powered	Yes	Knee	No	No	No	–	No	No
Tang *et al., ICMSE* [45]	Powered	Yes	Knee	Yes	No	No	–	No	No
Wang *et al., TMECH* [11]	Powered	Yes	Knee	No	No	Yes	–	No	No
Zanotto *et al., TRO* [10]	Powered	No	Knee	No	Yes	No	9 AB	No	No
Upper-Limb Exoskeletons									
Stienen *et al., JMD* [46]	Powered	Yes	Shoulder,elbow	No	No	No	>1 AB	No	No
Jarrasse *et al., TRO* [21]	Powered	Yes	Shoulder,elbow	No	Yes	Yes	10 AB	No	No
Ergin *et al., ICRA* [47]	Powered	Yes	Shoulder	Yes	No	No	2 AB	No	No
Vitiello *et al., TRO* [23]	Powered	Yes	Elbow	Yes	Yes	No	5 AB	No	No
Lenzi *et al., Mechatronics* [48]	Powered	Yes	Elbow	No	Yes	No	1 AB	No	No
Wu *et al., TMECH* [49]	Powered	Yes	Elbow,wrist	No	No	No	1 AB	No	No
Schiele, *IROS* [26]	Passive	Yes	Elbow	No	No	Yes	14 AB	Yes	Yes
Cempini *et al., TMECH* [25]	Powered	Yes	Finger,thumb	No	No	No	4 AB	No	No

the effective kinematic behavior diverges from the modeled one. From a design standpoint, it is challenging to implement a self-aligning mechanism that is lightweight, low friction, and robust enough to transfer the assistive torques through the powered joint axis while avoiding spurious forces and torques on the anatomical joint axis. Because the unmodeled mass, friction, and deformations of the self-aligning mechanism can impair its function, an experimental evaluation, including experiments under high assistive torque, is necessary.

The accuracy of predictions made using theoretical models depends on the modeling assumptions. The location of the user's anatomical joint axes, the exact position of the exoskeleton's braces and axes relative to the user's body, and the viscoelastic behavior of the wearer's limb at the interface with the exoskeleton all vary between subjects and even between sessions of exoskeleton use. Without knowledge of these variables, it is impossible to precisely predict the reduction of spurious forces and torques on the user's joints. More importantly, theoretical models cannot estimate how spurious forces and torques on the user's limb will affect the user's comfort. Similarly, theoretical models cannot predict how the spurious force and torques on the user's limb affect the user's performance with a powered exoskeleton. Thus, the effect of self-aligning mechanisms on the user's comfort and performance must be assessed experimentally.

We hypothesize that a lightweight, low-friction, and robust self-aligning mechanism will improve users' performance and perceived comfort during both fast, high-torque tasks and slow, low-torque tasks with a powered knee exoskeleton. This hypothesis was tested by asking 14 able-bodied subjects to perform assisted sit-to-stand transitions and trajectory tracking tasks using a unilateral powered knee exoskeleton with a self-aligning mechanism that can be mechanically locked [9]. All subjects experienced locked and unlocked conditions in a randomized order. The physical interaction at the pHRI was be measured using a six-axis force/torque sensor. Perceived comfort and effort were assessed using questionnaires.

II. BACKGROUND

A literature search on the topic of physical human-robot interaction in powered exoskeletons revealed that 24 powered exoskeletons with self-aligning mechanisms had been published—16 lower-limb exoskeletons and eight upper-limb exoskeletons (Table I). All upper-limb exoskeletons were tested with human subjects, although only two of them were tested with the self-aligning mechanism locked vs. unlocked. In contrast, only half of the powered lower-limb exoskeletons were tested with human subjects (six with only one subject and two with four subjects each). Notably, no powered lower-limb exoskeleton was tested with the self-aligning mechanism locked vs. unlocked.

Based on the literature search, performance with and without a self-aligning mechanism was never tested before. Also, with the exception of one upper-limb exoskeleton [26], subjective comfort was never tested in powered exoskeletons. A previous study assessed subjective comfort limits using an external apparatus to apply force to the human limbs

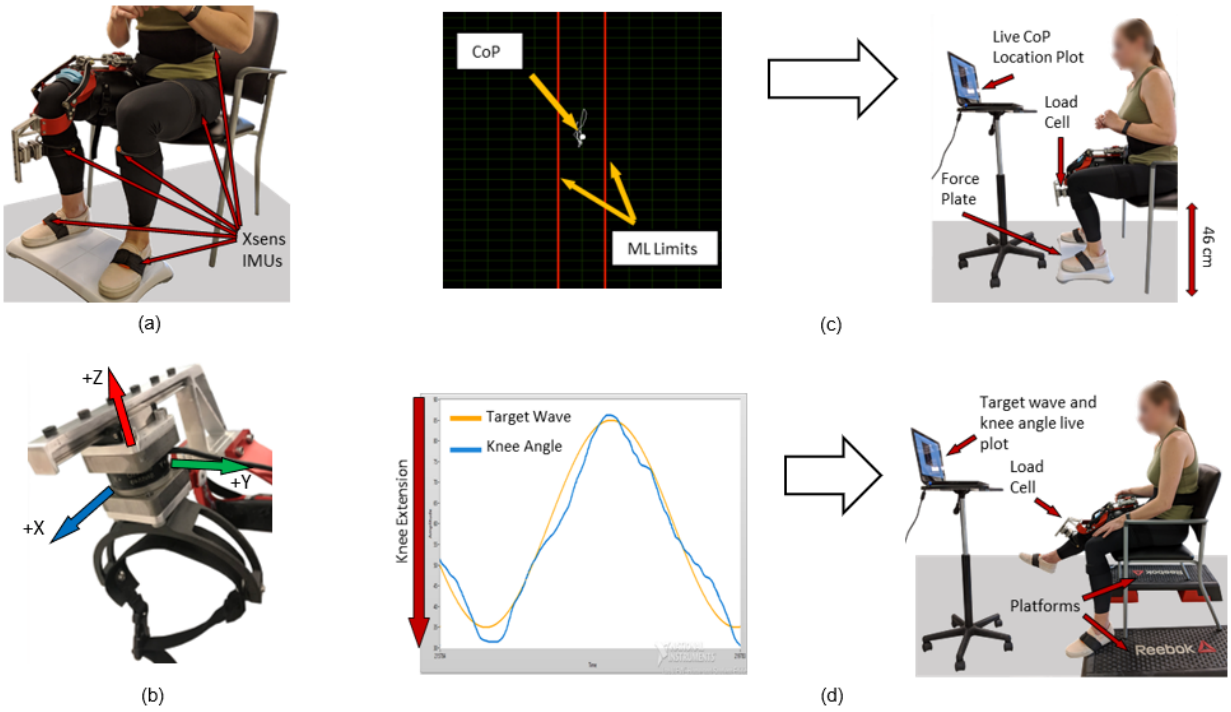

Fig. 1. Xsens IMUs that were placed on subjects' pelvis, left thigh, shanks, and ankles. Markers were also placed on the exoskeleton's thigh shell. In (b) the positioning and orientation of the load cell are shown. The load cell was added during experimentation and is not a permanent part of Utah ExoKnee. (c) Sit-to-stand transition test setup is shown. A wireless Wii board was used to track the center of pressure (CoP) of the subject during the sit-to-stand transitions. The subjects monitored the live location of their CoP on screen during the experiment. (d) Wave tracking test setup is shown. Platforms were placed under the chair legs to elevate the chair by approximately 15 cm in order to let the subject leg hang freely. The subjects monitored the live plot of the knee joint angle overlapped with a target wave on the screen during the experiment.

while participants stood still [27]. However, there was no powered exoskeleton involved, and subjects did not perform any movements. Thus, the spurious forces and torques experienced by the subjects during the experiment may have differed substantially from those that subjects would experience while using a powered exoskeleton. This literature search shows that there is no experimental demonstration of the effects of the self-aligning mechanism on comfort and performance in lower-limb exoskeletons.

Spurious forces and torques applied to the user's limbs were measured in four upper-limb and four lower-limb exoskeletons (Table I). Of these eight studies reporting spurious forces and torques, only one upper-limb exoskeleton study compared locked vs. unlocked configurations of a self-aligning mechanism. No lower-limb exoskeleton study showed spurious forces and torques with a self-aligning mechanism locked and unlocked. Thus, there is no experimental evidence suggesting that self-aligning mechanisms in lower-limb exoskeletons can match the reductions of spurious forces and torques predicted by theoretical models and benchtop studies.

III. Methods

A. Experimental Protocol

The experimental protocol was approved by the University of Utah Institutional Review Board. Written informed consent was provided to each subject before the experiment took place. The subjects provided written consent for the publication of their photos and videos. A total of fourteen able-bodied subjects were enrolled in the study (11 males, three females; 25.6 ± 4.16 years old, 176.1 ± 9.03 cm, and 71.4 ± 10.3 kg). This sample size matches that of the exoskeleton study with the largest number of subjects recruited in our literature search [26]. The subject information is presented in Table II.

Before the start of the data recording session, the subjects donned an inertial motion capture system to record their lower-limb kinematics (Xsens MVN Analyze, Xsens Technologies B.V., Enschede, Netherlands). The motion capture trackers were placed on both feet, shanks, and thighs (Fig. 1(a)). The motion capture system was calibrated during level-ground walking, as recommended by the manufacturer [28]. The calibration of the system starts with the subject standing in a neutral position: standing-upright, making sure that both arms are down, feet parallel, and about shoulder-width. On the experimenter's command, the subject starts walking at a normal pace. After a few seconds, the subject is asked to turn around and walk back at the same pace and take the initial position the subject started in, facing the same way. After the system calibration was completed, a powered knee exoskeleton was donned on the subject's right leg while sitting on a standard chair. After this setup was complete, the data recording started.

During each experimental session, the subjects performed two different tasks using the same powered knee exoskeleton. The first task, named *sit-to-stand*, consisted of 50 assisted sit-to-stand transitions from a standard-height chair (46 cm tall). While performing the transitions, the subjects stood on a force plate (Fig. 1(c)), which measured their center

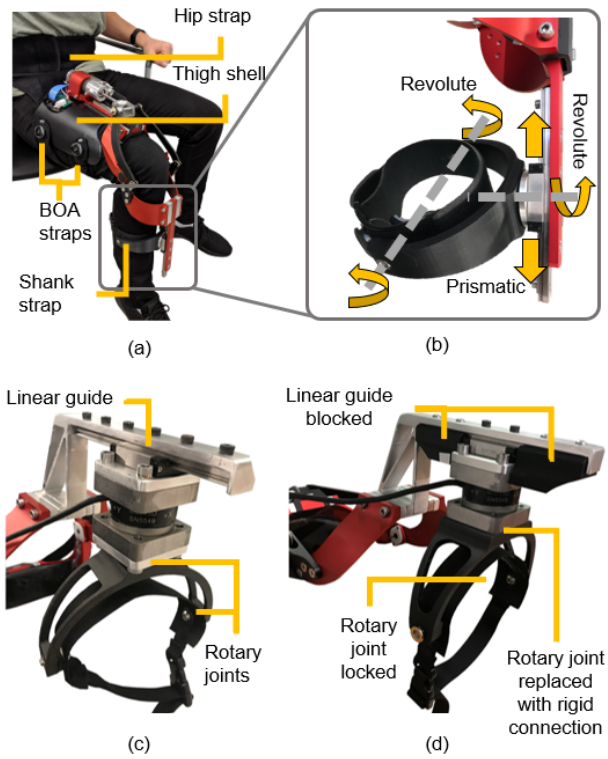

Fig. 2. (a) User wearing Utah ExoKnee. A hip strap wraps around the user's waist and thigh. The exoskeleton is attached to this hip strap by Velcro that covers the inside of the thigh shell. The exoskeleton is tightened around the thigh using BOA® straps. (b) Magnified view of Utah ExoKnee self-aligning mechanism. Three pDOFs are used in PRR configuration. (c) The Unlocked configuration during testing. The 3 pDOFs are allowed to move freely. (d) The Locked configuration during testing. The 3 pDOFs are blocked and not allowed to move. The linear guide of the prismatic pDOF is blocked by 3D-printed blocks that are attached to the frame placing the linear guide carriage in the center if the rail. The second, rotary pDOF is blocked by replacing the C-shaped cuff with one that connects rigidly by bolts to the load cell. The third pDOF is locked by tightening the bolts that act as the rotational axis.

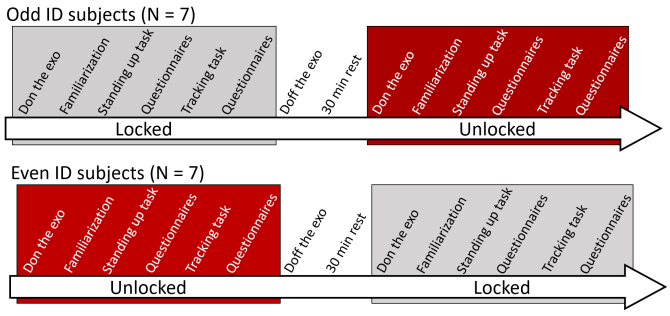

Fig. 3. Flow chart of human subject testing. The odd and even ID number subjects (Table II) defines which kinematic condition of the self-aligning mechanism each subject starts with. The subject ID numbers and, thus, the starting kinematic conditions, were assigned at random. The subjects were allowed to rest and recover for 30 minutes between the two testing conditions. While the subjects rested the experimenter reversed the kinematic condition of the self-aligning mechanism.

TABLE II
SUBJECT INFORMATION

Subject	Gender	Age	Height, cm	Weight, kg
S01	Male	39	175	70
S02	Male	26	178	70
S03	Male	26	185	84
S04	Male	24	165	57
S05	Female	25	165	64
S06	Male	24	185	75
S07	Male	22	180	91
S08	Male	26	172	66
S09	Male	22	180	72
S10	Male	22	188	75
S11	Male	26	185	73
S12	Female	25	157	52
S13	Female	25	172	68
S14	Male	26	178	82

of pressure (CoP) (Wii Balance Board, Nintendo®, Japan [29], [30]). The movement of the CoP in the mediolateral direction is an indication of sway and is commonly used to assess stability and balance in stroke patients during sit-to-stand transitions [31]. The subjects could see the location of their CoP on a monitor displaying a LabView graphical user interface (Fig. 1(c)). The subjects were asked to keep their CoP inside vertical boundary lines, which were shown in the graphical user interface. If their CoP moved outside of the defined boundaries (100 mm in each direction from the center of the board, in the medial-lateral direction), an acoustic cue was produced by the system. A training session consisting of 5 to 10 assisted sit-to-stand transitions in both self-aligning mechanism configurations were carried out before data recording took place.

In the second task, named *tracking*, the subjects were asked to track a sinusoidal wave with their knee joint while sitting in a chair, similar to the task shown in [32]. The chair was elevated from the ground by 15 cm to allow the subject's leg to hang freely in the air (Fig. 1(d)). The sinusoid wave frequency was set to 0.15 Hz with an amplitude of 25° and an offset of 60°. For this test, the powered knee exoskeleton was used in virtual stiffness mode. The objective of this task is to mimic the mobilization and strengthening exercises that are commonly performed for rehabilitation after ACL reconstruction surgery [33]. The joint stiffness was set to 0.1 Nm/deg, and the equilibrium point was at 40°. The reference sine wave was shown on a monitor and along with the knee joint measured by the position sensor embedded into the powered knee exoskeleton. To get the subjects accustomed to the setup, a 30-60 second wave tracking training session was carried out. The subjects were then asked to track the target sine wave for 5 minutes.

The tasks were carefully selected to provide different use-case scenarios for the powered exoskeleton and the self-aligning mechanism. One task is high-torque, weight-bearing, with the exoskeleton assisting the users and requires quick movements (*sit-to-stand*). The other task is low-torque, non-weight-bearing, with the exoskeleton resisting the users and requires slow movements (*tracking*).

The subjects repeated the two tasks using the same powered knee exoskeleton with the self-aligning mechanism in *Unlocked* and *Locked* configurations (Fig. 3). Subjects were blinded to the status of the self-aligning mechanism, and the specific goal of the experiment—comparing locked and unlocked conditions—was not explained to the subjects. Half of the subjects were randomly assigned to start the tests with the self-aligning mechanism *Unlocked*. The other half

started the experiments with the self-aligning mechanism *Locked*. After completing each task, the subjects filled out the NASA TLX questionnaire [34], rating 6 different fields: Mental Demand (*MD*); Physical Demand (*PD*); Temporal Demand (*TD*); Performance (*P*); Effort (*E*); Frustration (*F*). Additionally, the subjects rated the comfort (*C*) of the current exoskeleton on a visual analog scale with upper and lower limits of 0 and 100. Visual analog scales are commonly used in rehabilitation [35], and the same method was used in the only previous study that assessed comfort in a powered exoskeleton [26]. During the transition between the kinematic conditions, the subjects doffed the exoskeleton and were allowed to rest and walk as desired for 30 minutes (Fig. 3). While the subjects were resting, the experimenters changed the experimental condition: *[Unlocked* to *Locked]* or *[Locked* to *Unlocked]*, depending on the starting condition (Fig. 3). Both tasks and the familiarization session were then repeated under the new experimental condition.

B. Data Analysis and Statistical Design

Data analysis was conducted in MATLAB (MathWorks, USA). Data recorded by the exoskeleton during the standing-up task was segmented to include the standing-up motion only because the exoskeleton did not provide assistance during stand-to-sit transitions. The data was segmented by thresholding the position and velocity of the knee joint. The force plate data were segmented by thresholding the total force and the derivative of that force. Each standing-up repetition was then interpolated to 1000 data points. A zero-lag, low-pass fourth-order bidirectional Butterworth filter with 5 Hz cut-off frequency was applied to the joint position and velocity. The force and torque readings from the load-cell and the force plate data were not filtered. The data recorded by the exoskeleton during the tracking task did not require any segmentation because the data were analyzed as a whole. The performance analysis was conducted in MATLAB using embedded functions.

Statistical analysis was conducted to assess the outcome of the study using R (Free Software Foundation Inc., USA). In agreement with the proposed longitudinal study design, we used repeated measure ANOVA to assess statistical significance for the study outcomes, including user's comfort, NASA TLX scores, and task performance with respect to the study conditions. Specifically, the independent variables were the status of the self-aligning mechanism (i.e., locked vs. unlocked) and the task (i.e., standing-up, position tracking). The dependent variables were the measured interaction forces and torques (F_x, F_y, F_z, T_x, T_y, T_z), the NASA TLX scores (*MD, PD, TD, P, E, F)*, the comfort rating scale (*C*), and the objective performance metrics for the two tasks—the root mean square (RMS) error during tracking task and the standing-up task. Significance was set before the experiments at alpha $= 0.05$.

C. Powered Knee Exoskeleton and Related Controllers

For this study, we used a powered knee exoskeleton, namely Utah ExoKnee, which has been previously tested on the benchtop and with healthy subjects [9]. The Utah ExoKnee uses a compact and lightweight self-aligning mechanism with three passive degrees of freedom (pDOF). As shown in Fig. 2, the three pDOFs are arranged in prismatic-revolute-revolute (PRR) configuration and integrated in series with one active revolute DOF (knee flexion/extension). The prismatic pDOF is achieved using a low-friction linear guide connected to the shank segment of the exoskeleton. The linear guide carriage is attached to a custom rotary joint, which is a multi-turn joint with no mechanical stop. In turn, this custom rotational joint holds a C-shaped, 3D-printed frame with inlaid continuous carbon fiber, which connects to a flexible cuff through a perpendicular rotary DOF.

The thigh segment of the exoskeleton connects to the wearer's thigh through a flexible plastic molded thigh shell, the inner surface of which is lined with Velcro (Fig. 2(a)). The user wears a strap around their waist and thigh. The Velcro on the inner side of the thigh shell connects to the thigh portion of the strap (Fig. 2(a)), improving the physical connection between the exoskeleton and the user. The shell is tightened around the thigh using BOA® -system straps with magnetic buckles for quick donning (Fig. 2(a)). The thigh shell is flexible, allowing users with different thigh sizes/shapes to use the exoskeleton comfortably. The shank segment uses a C-shaped frame with an adjustable strap to adapt to different users and tighten securely to the limb (Fig. 2(a)).

A custom 3D-printed system can be mounted on the exoskeleton to lock the self-aligning mechanism, as shown in Fig. 2(d). When the locking system is mounted, no movements of the pDOFs are allowed. The linear guide of the prismatic pDOF is blocked by 3D-printed blocks that are attached to the frame placing the linear guide carriage in the center of the rail. The rotary pDOF is blocked by replacing the C-shaped cuff with one that connects rigidly by bolts to the load cell. The third pDOF is locked by tightening the bolts that act as the rotational axis. The locking system is lightweight (35g) and unobtrusive so that subjects do not notice its presence.

Dedicated controllers were used for the proposed tests. Specifically, for the standing-up test, the exoskeleton was set to provide assistive torque at the knee joint using the bio-inspired controller presented in [9]. For all experiments and subjects, we used a fixed peak assistive torque equal to 30 Nm. To start the standing-up movement, the experimenter switched the exoskeleton from transparent mode to standing-up mode using a graphical interface on the host computer connected to the exoskeleton via Wi-Fi. Once the exoskeleton knee angle reached 5° (i.e., extended knee position), the standing-up task was considered completed, and the controller automatically switched back to transparent mode, where the interaction torque was minimized by the closed-loop torque controller. For the sinewave tracking experiments, the exoskeleton was set to virtual-impedance mode. In this mode, the experimenter can select the desired equilibrium angle, stiffness, and damping of the joint, which are enforced by the closed-loop torque control. The two controllers have dedicated graphical user interfaces, which were shown to the user, shown in Fig. 1(c)(d).

The physical interaction between the subject and the exoskeleton was measured using a 6-axis load cell (M3713D, Sunrise Instruments, China). The load cell was placed between

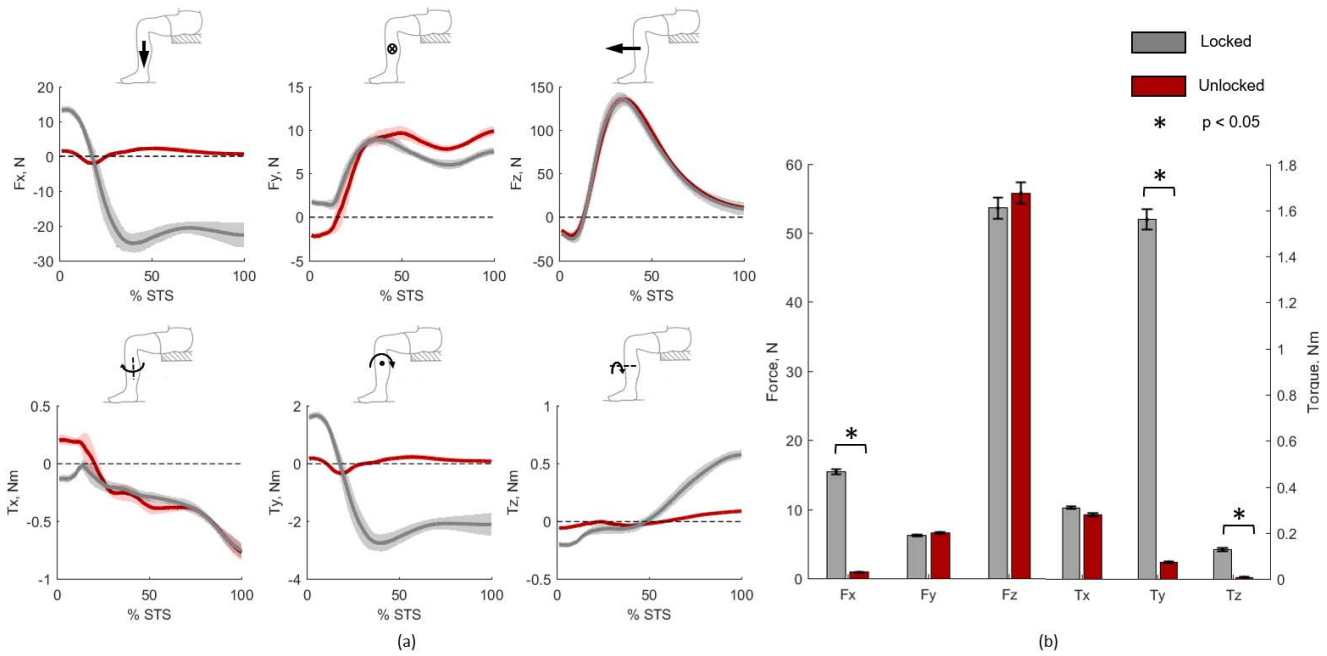

Fig. 4. (a) Mean values (solid lines) and standard deviations (shaded areas) of the interaction forces and torques between the subjects' shank and exoskeleton during the standing-up (STS) task are shown. (b) Bar plot of absolute values of average forces and torques is shown. The Unlocked and Locked conditions are compared. The Unlocked configuration is shown in red, and the Locked configuration is shown in grey. On the plots only the sit-to-stand movements are shown (no stand-to-sit movement). Error bars show standard error.

the linear guide carriage and the exoskeleton shank segment (Fig. 1(b)). As shown in Fig. 2, the user's limb is suspended in relation to the stiff 3D-printed cuff using a flexible brace [9]. Moreover, the load cell is connected to the 3D-printed cuff with 1/2″ (12.5 mm) thick steel plate (Fig. 2(c)). The steel plate prevents the deformation of the 3D printed cuff from inducing any measurable stress on the load cell, which was verified experimentally by the authors. Thus, tightening the brace does not affect the forces and torques sensed by the load cell. The strap was tightened to the upper comfort limit of each subject, and a verbal confirmation was obtained during each donning. We assumed this limit would stay consistent for each subject across the testing conditions. The load cell was zeroed using the same protocol for all subjects and test conditions. Specifically, the load cell was zeroed after the subjects were fit with the exoskeleton while subjects sat with their knees bent at about 90°, prior to data acquisition. The same procedure was carried out for the tracking task. The data from the load cell were acquired at 500 Hz using a National Instruments MyRIO board, which was synchronized with the exoskeleton's controller on-line. The embedded electronics of the exoskeleton recorded the output of all onboard sensors, including the angular position of the knee joint and the applied knee torque.

IV. Experimental Results

A. Physical Human-Robot Interaction

The physical interaction between the user and the robot was measured during all experiments using a force/torque sensor located at the shank. The interaction forces and torque profiles were averaged across all subjects and repetitions after time-normalization based on sit-to-stand transition time (Fig. 4(a)) or sine wave period (Fig. 5(a)) for both the *Unlocked* (solid red lines) and *Locked* conditions (solid grey lines). The average peaks of the forces and torques were also computed separately for each task (Fig. 4(b) and Fig. 5(b)). Only F_x, T_y, and T_z were compensated by the self-aligning mechanism. The interaction forces and torques were generally higher for the standing-up task than the position-tracking task. For both tests, the magnitudes of F_x, T_y, and T_z were visibly lower during the *Unlocked* conditions compared to the *Locked* conditions. Conversely, Fy, Fz, and T_x showed no visible difference in magnitude between *Locked* and *Unlocked* conditions. T_x and F_y increased towards the end of the sit-to-stand task when the subject was standing with the knee fully extended. For the standing-up task, the average peaks of F_x, T_y, and T_z (i.e., the reaction forces and torques compensated by pDOFs) were 95%, 97%, and 79% lower, respectively, for the *Unlocked* compared to the *Locked* condition. For the tracking task, the average peaks of F_x, T_y, and T_z were 97%, 96%, and 52% lower, respectively, for the *Unlocked* compared to the *Locked* conditions.

B. Perceived Comfort and Effort

The user's comfort was assessed using a 0 –100 visual analog scale, where 0 was described to subjects as *painful,* and 100 was described as "*the exoskeleton is not even worn.*" Comfort was rated by each subject for the self-aligning conditions and tasks separately (Fig. 6(a), (b)). The comfort score was averaged across subjects for the *Locked* (grey) and *Unlocked* (red) as well as for each task. The ANOVA analysis indicated that there were statistically significant differences

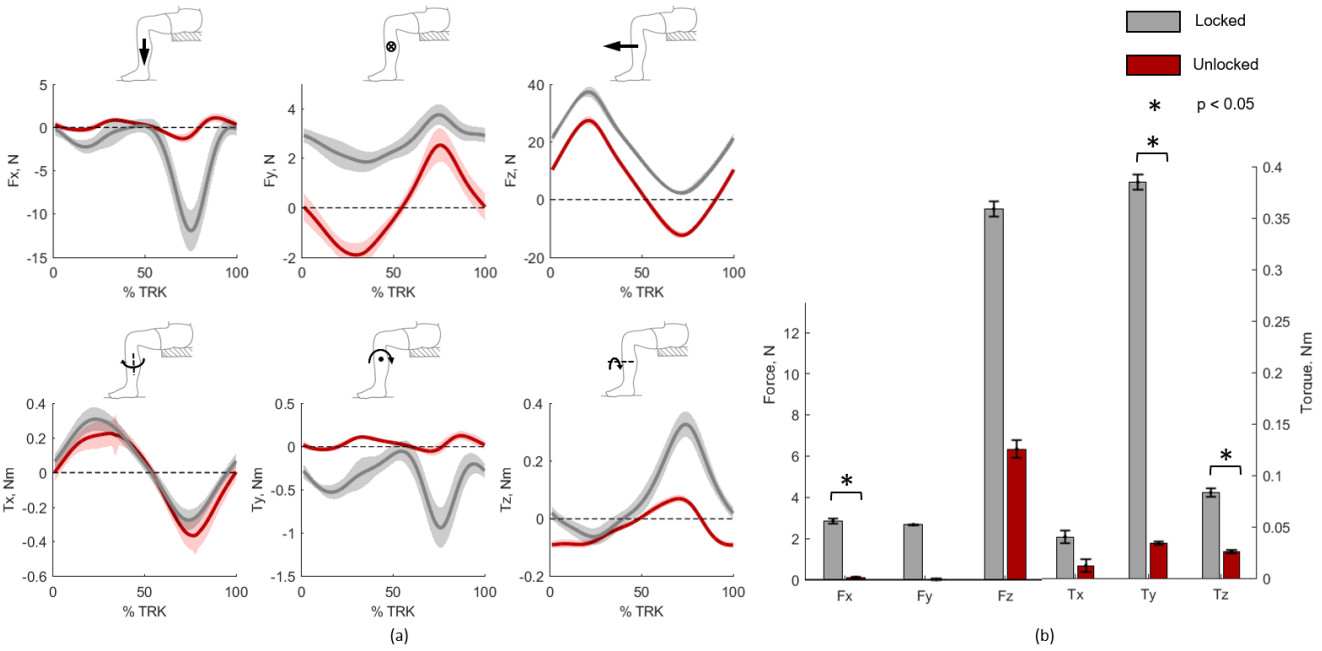

Fig. 5. (a) Mean values (solid lines) and standard deviations (shaded areas) of the interaction forces and torques between the subjects' shank and exoskeleton during the tracking *(TRK)* task are shown. (b) Bar plot of absolute values of average forces and torques is shown. The *Unlocked* and *Locked* conditions are compared. The *Unlocked* configuration is shown in red, and the *Locked* configuration is shown in grey. The data was segmented to one sine wave period and averaged across trials and subjects. Error bars show standard error.

in the comfort rating between both the *Locked* and *Unlocked* conditions ($p = 0.0371$) and the tasks ($p = 0.0076$). The statistical analysis is summarized in Table III. The mean comfort ratings during the standing-up task were 58.2 and 67.1 for *Locked* and *Unlocked* conditions, respectively (Fig. 6(a)). Thus, the comfort rating improved by 15.3% during the *Unlocked* condition, compared to *Locked*. The mean comfort ratings during the tracking task were 69.6 and 77.5 for *Locked* and *Unlocked* conditions, respectively (Fig. 6(b)). Thus, comfort was improved by 11.4% during the *Unlocked* condition, compared to *Locked*. The comfort rating was 21.8% higher during the tracking task than during the standing-up task.

NASA TLX (Task Load Index) was used to assess subjects' task load and demand in 6 different fields. The NASA TLX task load ratings were averaged across subjects for each of the six fields (Fig. 6(c), (d)). The ANOVA analysis showed no statistically significant differences in any NASA TLX ratings between the *Locked* and *Unlocked* conditions.

C. Task Performance

Performance during the standing-up task was assessed by analyzing the position of the center of pressure during the execution of the assisted movement. The trajectories of the center of pressure (CoP) were analyzed for all the standing-up repetitions and all subjects (Fig. 8). The RMS of the medial-lateral CoP location averaged across all subjects for the *Locked* conditions was 34.0 mm (Fig. 7(a)), compared to 25.8 mm for the *Unlocked* condition. Thus, the RMS error of the medial-lateral CoP location was 32% higher for the *Locked* condition compared to the *Unlocked* condition. The peaks of the medial-lateral CoP location averaged across all subjects were 58.8 mm and 41.8 mm for the *Locked* and *Unlocked* conditions, respectively. Paired t-tests showed that the RMS and peaks of the medial-lateral CoP location were statistically different between the *Locked* and *Unlocked* conditions ($p = 4.6877e-6$ for RMS, $p = 1.4731e-6$ for peak).

Performance during the tracking task was assessed by calculating the difference between the desired knee position and the measured knee position, which were shown to the subject in the graphical interface (Fig. 1). The RMS errors were computed for each subject (Fig. 7(b)). The RMS averaged across subjects were 5.99° and 4.33° for the *Locked* and *Unlocked* conditions, respectively. Thus, the RMS was, on average, 38% lower for the *Unlocked* condition compared to the *Locked* condition. A paired t-test found the observed difference between conditions to be statistically significant ($p = 0.0021$).

V. Discussion

A. Human Experiments

Misalignments between the exoskeleton joints and the anatomical axes of rotation are inevitable [9] and can lead to undesired, spurious forces and torques on the wearer's skin and articulation [21], [11]. Theoretical models [21], [13], [11] suggest that self-aligning mechanisms have the potential to reduce the spurious forces and torques, and numerous self-aligning mechanisms have been developed [1], [5], [14]–[17]. However, experiments validating the efficacy of this design solution are lacking, and the effect of self-aligning mechanisms on comfort and performance has never been assessed in lower-limb exoskeletons (Table I). Because theoretical models cannot assess the user's comfort and performance, experiments

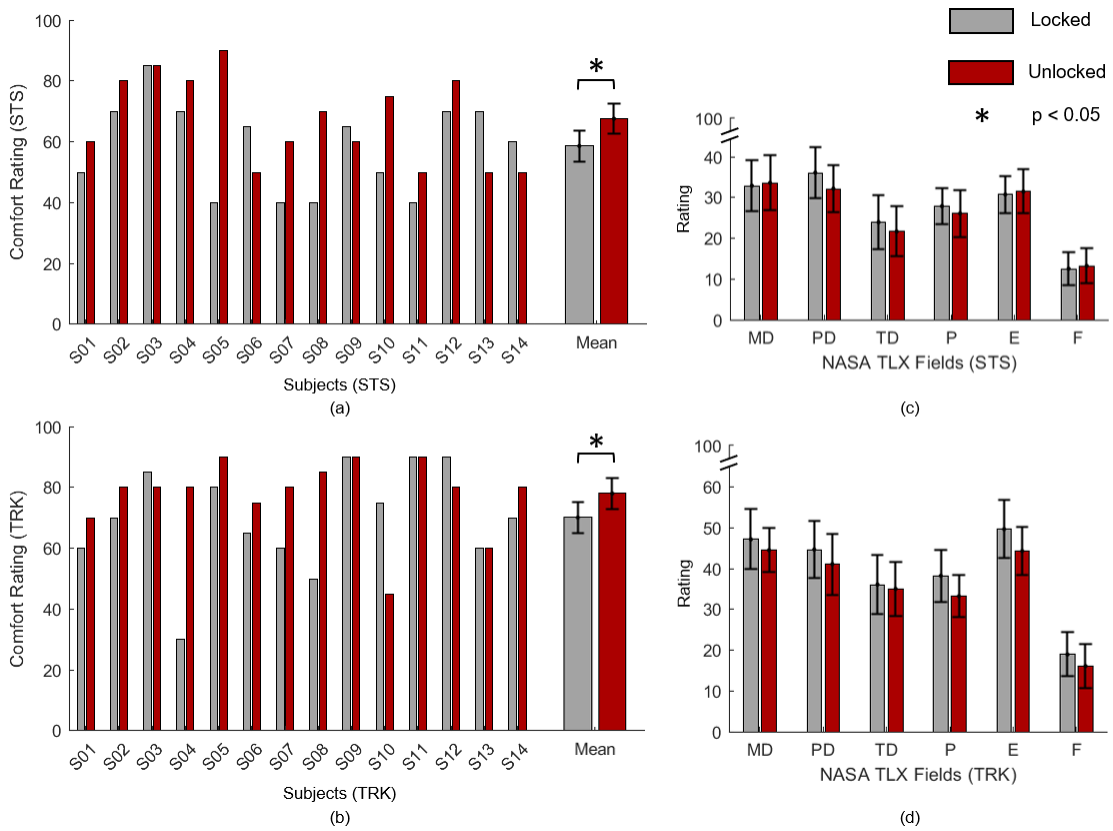

Fig. 6. The comfort scale ratings of each subject and the subject mean are shown in the left column. (a) The standing up (STS) task responses are shown. (b) The tracking (TRK) task responses are shown. The comfort scale ranges from 0, described as painful, to 100, described as if the exoskeleton was not even worn. Right column shows NASA TLX scale ratings averaged by fields across all subjects: Mental Demand *(MD)*; Physical Demand *(PD)*; Temporal Demand *(TD)*; Performance *(P)*; Effort *(E)*; Frustration *(F)*. (c) The standing up task responses are shown. (d) The tracking task responses are shown. The rating scales range from 0 (low), to 100 (high). The *Locked* condition is shown in grey and the *Unlocked* condition is shown in red. Error bars show standard error.

with a significant number of subjects are necessary. This study presents the first demonstration that a self-aligning mechanism can significantly improve comfort and performance. Improvements were shown in N = 14 subjects performing slow and fast assisted activities with a powered exoskeleton.

The experimental protocol included two tasks: standing-up while assisted by the exoskeleton and tracking a desired position against a virtual impedance field generated by the powered exoskeleton. A future clinical trial will use the powered knee exoskeleton to assist standing-up in hemiparetic subjects. Another future clinical trial will use the powered knee exoskeleton to perform position tracking for robot-mediated rehabilitation after anterior cruciate ligament reconstruction surgery. Our results show that the proposed self-aligning mechanism significantly improves comfort and performance while reducing the spurious forces and torques on the user for both tasks. Because comfort and performance are paramount, this study strongly supports the use of self-aligning mechanisms in future clinical trials with powered knee exoskeletons.

This study demonstrates the efficacy of self-aligning mechanisms in improving comfort and performance during sit-to-stand and position tracking tasks with a powered knee exoskeleton. However, we should carefully consider the key design features of the proposed self-aligning mechanism before generalizing the results of this study to other powered exoskeletons. The mass of the self-aligning mechanism, which is not considered in theoretical models, has a critical, negative effect on its function. For example, gravity can cause the passive joints of a self-aligning mechanism to slide and reach its mechanical end-stop, effectively impairing the self-aligning function. Similarly, inertial forces and torques due to the mass of the self-aligning mechanism can cause its passive joints to move during activity. These unmodeled and uncontrolled movements are likely to limit the potential reduction of spurious forces and torques as well as to cause discomfort to the user. Therefore, we believe that the relatively small mass of the proposed self-aligning mechanism (190 g, which is ∼5.3% of the overall exoskeleton mass [9]) was critical to achieving the observed improvements in comfort and performance.

Reducing the mass of a self-aligning mechanism without impairing its function under load is challenging. The passive joints of a self-aligning mechanism must be able to move freely while transferring the assistive torque. For example, the prismatic joint shown in Fig. 2(c) must be able to slide freely while transferring the force F_z (Fig. 1(b)) so that the powered exoskeleton can provide assistive or resistive torques at the user's knee joint. In our design, we used a relatively large linear guide compared to other systems (150 g, 3.5 kN max load) (Table. I). Although using a smaller and lighter linear guide would have reduced the overall mass, it could

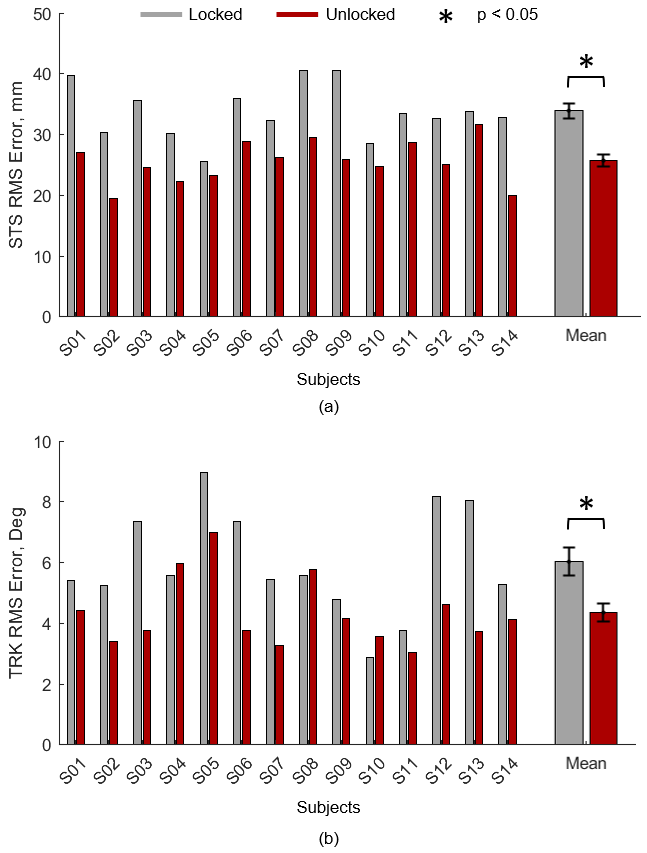

Fig. 7. The RMS error between perfect medial-lateral balance and the CoP position during standing up (STS) task are shown in (a). The RMS errors between the measured knee angle and the target wave during the tracking (TRK) task are shown in (b). The two kinematic conditions were compared: the self-aligning mechanism *Locked* and *Unlocked*. The *Locked* condition is shown in grey and the Unlocked condition is shown in red. In addition to RMS errors of each subject's performance, the means of all RMS errors are shown. A paired t-test has established statistical significance between the kinematic condition of the self-aligning mechanism and the RMS error values (STS: $p = 4.6877e-06$, TRK: $p = 0.0021$). Error bars show standard error.

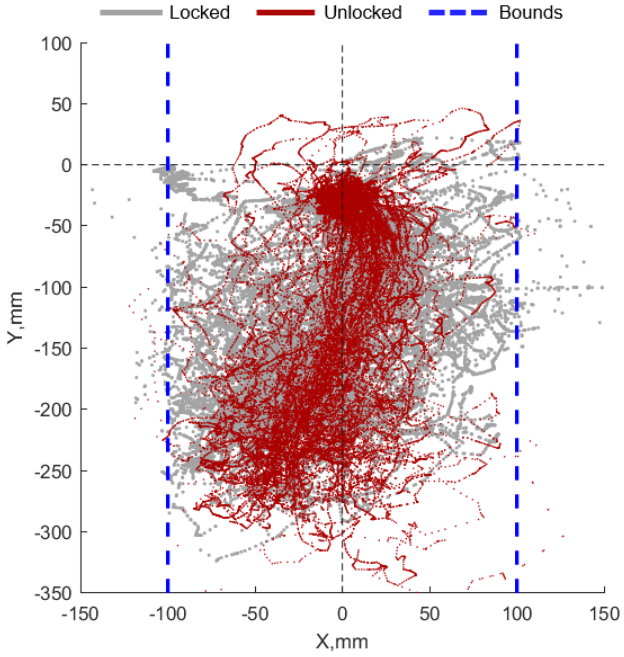

Fig. 8. The center of pressure (CoP) plot of all trials and subjects is shown. Only sit-to-stand movement is presented. The two kinematic conditions were compared: the self-aligning mechanism *Locked* and *Unlocked*. The *Locked* condition is shown in grey and the *Unlocked* condition is shown in red. The bounds that the subjects were asked to stay in are shown as vertical blue dashed lines.

have increased friction, which could impair the movement of the passive joints under load. Notably, the symmetric design of the powered exoskeleton has a critical effect on the function of the self-aligning mechanism. The symmetric design minimizes the torque on the linear guide, allowing for both the mass and the friction of the self-aligning mechanism to be minimized. Similarly, the symmetric design reduces the load that the linkages of the self-aligning mechanism must withstand. This load reduction is critical because deformations in the linkages of the self-aligning mechanism may impair the ability of its passive joints to move freely under load.

The comfort and effort during each experimental condition were assessed using questionnaires filled out by the subjects at the end of each test (i.e., standing-up and tracking tasks, with *Locked* and *Unlocked* exoskeleton). Our results show that the presence of the self-aligning mechanism significantly improves comfort during both the standing-up and the tracking task. Interestingly, the tracking task was significantly more comfortable than the standing-up task. This result may be explained by the fact that the spurious forces and torques were greater during the standing-up task than the tracking tasks. Thus, our study suggests that there is a correlation between the spurious forces and torques and the user's comfort. A previous study [27] suggests that the comfort limit for the shank is 702 ± 220 N, which greatly exceeds the average peak force measured in our experiments during the *Locked* condition, which was ∼30 N. Our results suggest that these interaction forces and torques were large enough for the subjects to feel less comfortable during the *Locked* conditions than during *Unlocked* condition (Fig. 6). Cumulatively, our results confirm our hypothesis that reducing the spurious forces and torques leads to improved comfort.

Performance during the standing-up task was assessed using the root-mean-square error between the CoP and the midline of the force plate and the maximum deviation of the CoP from the midline. Our results show that both performance metrics were significantly better (up to 32%) in the presence of the self-aligning mechanism (i.e., *Unlocked* condition). In general, the position of the center of pressure was biased towards the right side (Fig. 8)—the side wearing the exoskeleton. This result is likely due to the additional mass of the exoskeleton, which was located on the right side of the subjects' body. Performance during the tracking task was assessed using the RMS error between the target wave and measured knee angle. The RMS error was significantly lower in the *Unlocked* condition than the *Locked* conditions (38%). A previous upper-limb exoskeleton study [26], in which the authors investigated different attachment pressures with the self-aligning mechanism locked and unlocked, showed that the unlocked condition was preferred at the optimum interface attachment pressure because of improved tracking performance. Cumulatively, our

TABLE III
RESULTS OF THE STATISTICAL ANALYSIS

Parameters		Kinematic Condition		Task	
Load-cell Measured F/T	mean(F_x)	**F(1,53) = 32.7**	**p < 0.00001**	F(1,53) = 0.172	p > 0.05
	mean(F_y)	F(1,53) = 0.375	p > 0.05	F(1,53) = 1.78	p > 0.05
	mean(F_z)	F(1,53) = 1.18	p > 0.05	**F(1,53) = 39.0**	**p < 0.00001**
	mean(T_x)	F(1,53) = 0.618	p > 0.05	F(1,53) = 0.104	p > 0.05
	mean(T_y)	**F(1,53) = 42.2**	**p < 0.00001**	**F(1,53) = 5.45**	**p < 0.05**
	mean(T_z)	**F(1,53) = 16.9**	**p < 0.001**	F(1,53) = 0.631	p > 0.05
NASA TLX	Mental Demand *(MD)*	F(1,53) = 0.0226	p > 0.05	F(1,53) = 3.86	p > 0.05
	Physical Demand *(PD)*	F(1,53) = 0.324	p > 0.05	F(1,53) = 1.76	p > 0.05
	Temporal Demand *(TD)*	F(1,53) = 0.0645	p > 0.05	F(1,53) = 3.72	p > 0.05
	Performance *(P)*	F(1,53) = 0.385	p > 0.05	F(1,53) = 2.56	p > 0.05
	Effort *(E)*	F(1,53) = 0.161	p > 0.05	**F(1,53) = 7.55**	**p < 0.01**
	Frustration *(F)*	F(1,53) = 0.0509	p > 0.05	F(1,53) = 0.956	p > 0.05
Comfort Score *(0-100)*		**F(1,53) = 4.57**	**p < 0.05**	**F(1,53) = 7.70**	**p < 0.01**
Sit-to-stand Tracking	$RMS\ (X_{ideal} - X_{meas})$	**paired t-test: p < 0.00001**		N/A	
	$RMS\ (\theta_{target} - \theta_{meas})$	**paired t-test: p < 0.01**		N/A	

results agree with this previous study and suggest that self-aligning mechanisms can improve the user's performance with a powered exoskeleton.

NASA TLX was used to assess the task load of the subjects during the experiments. Our analysis shows that there are no statistically significant differences in the NASA TLX ratings between the *Locked* and *Unlocked* conditions. However, there was a statistically significant difference in the *Effort* (E) rating between the standing-up and tracking tasks. This shows that the subjects perceive the tracking task to be more challenging than the standing-up task.

Our results show that the presence of the self-aligning mechanism (i.e., *Unlocked* condition) leads to a significant decrease in the average values for F_x, T_y, and T_z during both standing-up and tracking tasks. (Fig. 4, Fig. 5). This reduction is explained by the fact that the self-aligning mechanism implemented in the Utah ExoKnee [9] comprises three pDOFs, allowing translational movements along the X-axis (Fig. 2) and rotational movements around the Y- and Z-axes. This result shows that the proposed self-aligning mechanism has a significant effect on spurious forces and torques. We expect that regardless of the specific kinematics or mechanical implementation, a self-aligning mechanism should be able to achieve similar comfort and performance improvement, provided it can show a similar reduction in spurious forces and torques.

The averages of F_y and F_z are similar for the *Locked* and *Unlocked* conditions during the standing-up task but not for the tracking task (Fig. 4(b), Fig. 5(b)). During the tracking task, F_y and F_z follow similar trajectories (Fig. 5(a)). However, during the *Unlocked* condition, the data is offset compared to the *Locked* condition. This variation in F_y and F_z between conditions may have been caused by the position of the loadcell with respect to the active joint of the powered exoskeleton - this position may change when the self-aligning mechanism is in the *Unlocked* condition because the loadcell can slide along the frame of the exoskeleton. Interestingly, during the standing-up task, the average value of F_z is slightly higher in the *Unlocked* than the *Locked* condition. With the *Unlocked* system, only F_z contributes to generating the desired flexion/extension torque on the user's knee. In contrast, with the *Locked* system, both F_z and T_y contribute to transfer the desired knee flexion/extension torque to the user's knee. This result could mean a purer translation of torque between the exoskeleton and the human limb during the *Unlocked* condition.

B. Limitations

Our results show that the self-aligning mechanism implemented in the Utah ExoKnee significantly improves comfort and performance while reducing spurious forces and torques during sit-to-stand and position tracking tasks. However, it is not clear if these results can be generalized to other joints, other tasks, or other powered exoskeletons. The self-aligning mechanism in the Utah ExoKnee was designed to be particularly lightweight (190g, 5.3% of the overall device weight) and small. It is possible that a larger and heavier self-aligning mechanism would not produce the same results. Similarly, it is possible that the application of self-aligning mechanisms to other joints or to other tasks would not produce the same results. To address this issue, we are currently investigating the effects of a similar self-aligning mechanism in a powered hip exoskeleton during walking [36]. Self-aligning mechanisms have mostly been considered in the actuated plane. The Utah ExoKnee has one pDOF that compensates for torque in a non-actuated plane (T_z). In addition, the interaction force along the Y-axis (F_y) and the torque about the X-axis (T_x) are not compensated by a pDOF in Utah ExoKnee. Our results show that the addition of pDOFs in the actuated plane is enough to significantly reduce the interaction forces and torques. However, it is important to consider the variability of the limb shape between users. Given the planar nature of the mechanism, it should be possible to implement additional pDOFs while transmitting torque in the sagittal plane, as done in [5]. However, it is challenging to add pDOFs in other planes in high-load transmission systems without increased structural complexity, size, and weight.

The self-aligning mechanism weighs 190 g, which is ∼5.3% of the overall exoskeleton mass [9]. While the added mass is far from the center of mass, we believe it is too small to add significant mechanical impedance to the exoskeleton.

During the experiments, the standing-up assistance mode was manually activated by the experimenter. Although the subject could decide when to stand up and stand-up at their self-selected speed, it would be valuable for the exoskeleton to automatically detect the user's intention to transition into the sit-to-stand mode, as previously done in powered prostheses [37]. We expect that the standing-up controller used with the powered exoskeleton may affect the user's performance. However, we do not expect the controller to affect the results of the comparison between *Locked* and *Unlocked* conditions.

Although a thorough explanation of the NASA TLX ratings was given to the subjects before they answered the questionnaire, subjects were often confused and seemed to find the definitions unclear when applied to the tasks performed in this study. Our observations suggest that the NASA TLX rating scale may not be sensitive enough for the tasks performed in this study. It would be beneficial to develop a rating scale to assess the physical and mental effort during the use of wearable robots.

In this study, we used a visual analog scale with the lower and upper limits marked as 0 and 100. The subjects were verbally informed about the meaning of the upper and lower limits of the scale. Although this method has been used before in rehabilitation [35], it has not been commonly used with powered exoskeletons because the user's comfort is not typically assessed (Table I). Because no other study has ever assessed comfort and performance with a self-aligning mechanism in any population, we only recruited healthy subjects. Future studies should examine whether comfort and performance are improved in individuals with a physical disability. Based on the results of this study, we plan to use the self-aligning mechanism in future experiments testing sit-to-stand assistance with hemiparetic subjects and robot-mediated rehabilitation with individuals who underwent reconstruction surgery of the anterior cruciate ligament.

VI. Conclusion

Powered exoskeletons aim to improve the movement ability of their human users. To accomplish this goal, powered exoskeletons must physically interact with the user safely and comfortably. Misalignments between the exoskeleton's powered joint and the user's anatomical joint have proved to be a challenge because of the resulting undesired torque and forces on the user's limb. Our tests with 14 subjects standing-up and performing a position tracking task with a powered knee exoskeleton show that a self-aligning mechanism can address the negative effects of the misalignment. With the self-aligning mechanism, the interaction forces and torques up to 97%, the comfort increased by 15.3%, and the performance improved by 38%. Thus, this study shows that lightweight, compact, and robust self-aligning mechanisms can improve both comfort and performance when using a powered knee exoskeleton for high-torque, high-power tasks such as sit-to-stand transitions and low-torque, low-power tasks such as tracking the desired position under a virtual impedance field.

References

[1] M. A. Ergin and V. Patoglu, "A self-adjusting knee exoskeleton for robot-assisted treatment of knee injuries," in *Proc. IEEE/RSJ Int. Conf. Intell. Robots Syst.*, Sep. 2011, pp. 4917–4922.

[2] L. M. Mooney, E. J. Rouse, and H. M. Herr, "Autonomous exoskeleton reduces metabolic cost of human walking during load carriage," *J. NeuroEngineering Rehabil.*, vol. 11, no. 1, p. 80, 2014.

[3] T. Lenzi, D. Zanotto, P. Stegall, M. C. Carrozza, and S. K. Agrawal, "Reducing muscle effort in walking through powered exoskeletons," in *Proc. Annu. Int. Conf. IEEE Eng. Med. Biol. Soc.*, Aug. 2012, pp. 3926–3929.

[4] S. Lefmann, R. Russo, and S. Hillier, "The effectiveness of robotic-assisted gait training for paediatric gait disorders: Systematic review," *J. NeuroEngineering Rehabil.*, vol. 14, no. 1, pp. 1–10, Dec. 2017.

[5] L. Saccares, I. Sarakoglou, and N. G. Tsagarakis, "IT-knee: An exoskeleton with ideal torque transmission interface for ergonomic power augmentation," in *Proc. IEEE/RSJ Int. Conf. Intell. Robots Syst. (IROS)*, Oct. 2016, pp. 780–786.

[6] H. Kazerooni, "Exoskeletons for human power augmentation," in *Proc. IEEE/RSJ Int. Conf. Intell. Robots Syst.*, Aug. 2005, pp. 3459–3464.

[7] S. Kim, M. A. Nussbaum, M. I. Mokhlespour Esfahani, M. M. Alemi, S. Alabdulkarim, and E. Rashedi, "Assessing the influence of a passive, upper extremity exoskeletal vest for tasks requiring arm elevation: Part I—'Expected' effects on discomfort, shoulder muscle activity, and work task performance," *Appl. Ergonom.*, vol. 70, pp. 315–322, Jul. 2018.

[8] M. A. Lafortune, P. R. Cavanagh, H. J. Sommer, and A. Kalenak, "Three-dimensional kinematics of the human knee during walking," *J. Biomechanics*, vol. 25, no. 4, pp. 347–357, Apr. 1992.

[9] S. V. Sarkisian, M. K. Ishmael, G. R. Hunt, and T. Lenzi, "Design, development, and validation of a self-aligning mechanism for high-torque powered knee exoskeletons," *IEEE Trans. Med. Robot. Bionics*, vol. 2, no. 2, pp. 248–259, May 2020.

[10] D. Zanotto, Y. Akiyama, P. Stegall, and S. K. Agrawal, "Knee joint misalignment in exoskeletons for the lower extremities: Effects on User's gait," *IEEE Trans. Robot.*, vol. 31, no. 4, pp. 978–987, Aug. 2015.

[11] D. Wang, K.-M. Lee, J. Guo, and C.-J. Yang, "Adaptive knee joint exoskeleton based on biological geometries," *IEEE/ASME Trans. Mechatronics*, vol. 19, no. 4, pp. 1268–1278, Aug. 2014.

[12] A. Schiele and F. C. T. van der Helm, "Kinematic design to improve ergonomics in human machine interaction," *IEEE Trans. Neural Syst. Rehabil. Eng.*, vol. 14, no. 4, pp. 456–469, Dec. 2006.

[13] M. Cempini, S. M. M. De Rossi, T. Lenzi, N. Vitiello, and M. C. Carrozza, "Self-alignment mechanisms for assistive wearable robots: A kinetostatic compatibility method," *IEEE Trans. Robot.*, vol. 29, no. 1, pp. 236–250, Feb. 2013.

[14] V. A. D. Cai, P. Bidaud, V. Hayward, F. Gosselin, and E. Desailly, "Self-adjusting, isostatic exoskeleton for the human knee joint," in *Proc. Annu. Int. Conf. IEEE Eng. Med. Biol. Soc.*, Aug. 2011, pp. 612–618.

[15] B. Celebi, M. Yalcin, and V. Patoglu, "AssistOn-knee: A self-aligning knee exoskeleton," in *Proc. IEEE/RSJ Int. Conf. Intell. Robots Syst.*, Nov. 2013, pp. 996–1002.

[16] J.-H. Kim *et al.*, "Design of a knee exoskeleton using foot pressure and knee torque sensors," *Int. J. Adv. Robotic Syst.*, vol. 12, no. 8, p. 112, Aug. 2015.

[17] D. J. Hyun, H. Park, T. Ha, S. Park, and K. Jung, "Biomechanical design of an agile, electricity-powered lower-limb exoskeleton for weight-bearing assistance," *Robot. Auto. Syst.*, vol. 95, pp. 181–195, Sep. 2017.

[18] K. Junius, M. Degelaen, N. Lefeber, E. Swinnen, B. Vanderborght, and D. Lefeber, "Bilateral, misalignment-compensating, full-DOF hip exoskeleton: Design and kinematic validation," *Appl. Bionics Biomechanics*, vol. 2017, pp. 1–14, Jul. 2017.

[19] F. Giovacchini *et al.*, "A light-weight active orthosis for hip movement assistance," *Robot. Auto. Syst.*, vol. 73, pp. 123–134, Nov. 2015.

[20] N. d'Elia *et al.*, "Physical human-robot interaction of an active pelvis orthosis: Toward ergonomic assessment of wearable robots," *J. NeuroEngineering Rehabil.*, vol. 14, no. 1, pp. 1–14, Dec. 2017.

[21] N. Jarrasse and G. Morel, "Connecting a human limb to an exoskeleton," *IEEE Trans. Robot.*, vol. 28, no. 3, pp. 697–709, Jun. 2012.

[22] A. H. A. Stienen, E. E. G. Hekman, F. C. T. van der Helm, and H. van der Kooij, "Self-aligning exoskeleton axes through decoupling of joint rotations and translations," *IEEE Trans. Robot.*, vol. 25, no. 3, pp. 628–633, Jun. 2009.

[23] N. Vitiello *et al.*, "NEUROExos: A powered elbow exoskeleton for physical rehabilitation," *IEEE Trans. Robot.*, vol. 29, no. 1, pp. 220–235, Feb. 2013.
[24] J. C. Perry, J. Rosen, and S. Burns, "Upper-limb powered exoskeleton design," *IEEE/ASME Trans. Mechatronics*, vol. 12, no. 4, pp. 408–417, Aug. 2007.
[25] M. Cempini, M. Cortese, and N. Vitiello, "A powered finger–thumb wearable hand exoskeleton with self-aligning joint axes," *IEEE/ASME Trans. Mechatronics*, vol. 20, no. 2, pp. 705–716, Apr. 2015.
[26] A. Schiele, "Ergonomics of exoskeletons: Subjective performance metrics," in *Proc. IEEE/RSJ Int. Conf. Intell. Robots Syst.*, Oct. 2009, pp. 480–485.
[27] M. B. Yandell, D. M. Ziemnicki, K. A. McDonald, and K. E. Zelik, "Characterizing the comfort limits of forces applied to the shoulders, thigh and shank to inform exosuit design," *PLoS One*, vol. 15, no. 2, pp. 1–12, 2020.
[28] J.-T. Zhang, A. C. Novak, B. Brouwer, and Q. Li, "Concurrent validation of Xsens MVN measurement of lower limb joint angular kinematics," *Physiological Meas.*, vol. 34, no. 8, pp. N63–N69, Aug. 2013.
[29] F. Sgrò, G. Monteleone, M. Pavone, and M. Lipoma, "Validity analysis of wii balance board versus baropodometer platform using an open custom integrated application," *AASRI Procedia*, vol. 8, pp. 22–29, Jan. 2014.
[30] H. L. Bartlett, L. H. Ting, and J. T. Bingham, "Accuracy of force and center of pressure measures of the Wii Balance Board," *Gait Posture*, vol. 39, no. 1, pp. 224–228, Jan. 2014.
[31] P.-T. Cheng, M.-Y. Liaw, M.-K. Wong, F.-T. Tang, M.-Y. Lee, and P.-S. Lin, "The sit-to-stand movement in stroke patients and its correlation with falling," *Arch. Phys. Med. Rehabil.*, vol. 79, no. 9, pp. 1043–1046, Sep. 1998.
[32] R. Ronsse, N. Vitiello, T. Lenzi, J. van den Kieboom, M. C. Carrozza, and A. J. Ijspeert, "Human–robot synchrony: Flexible assistance using adaptive oscillators," *IEEE Trans. Biomed. Eng.*, vol. 58, no. 4, pp. 1001–1012, Apr. 2011.
[33] B. D. Beynnon *et al.*, "Rehabilitation after anterior cruciate ligament reconstruction: A prospective, randomized, double-blind comparison of programs administered over 2 different time intervals," *Amer. J. Sports Med.*, vol. 33, no. 3, pp. 347–359, Mar. 2005.
[34] S. G. Hart and L. E. Staveland, "Development of NASA-TLX (task load index): Results of empirical and theoretical research," *Adv. Psychol.*, vol. 52, pp. 139–183, Apr. 1988.
[35] P. Kersten, A. A. Küçükdeveci, and A. Tennant, "The use of the Visual Analo gue Scale (VAS) in rehabilitation outcomes," *J. Rehabil. Med.*, vol. 44, no. 7, pp. 609–610, 2012.
[36] M. K. Ishmael, M. Tran, and T. Lenzi, "ExoProsthetics: Assisting above-knee amputees with a lightweight powered hip exoskeleton," in *Proc. IEEE 16th Int. Conf. Rehabil. Robot. (ICORR)*, Jun. 2019, pp. 925–930.
[37] H. A. Varol, F. Sup, and M. Goldfarb, "Multiclass real-time intent recognition of a powered lower limb prosthesis.," *IEEE Trans. Biomed. Eng.*, vol. 57, no. 3, pp. 542–551, Mar. 2010.
[38] Y. Lee *et al.*, "Biomechanical design of a novel flexible exoskeleton for lower extremities," *IEEE/ASME Trans. Mechatronics*, vol. 22, no. 5, pp. 2058–2069, Oct. 2017.
[39] K. Junius, N. Lefeber, E. Swinnen, B. Vanderborght, and D. Lefeber, "Metabolic effects induced by a kinematically compatible hip exoskeleton during STS," *IEEE Trans. Biomed. Eng.*, vol. 65, no. 6, pp. 1399–1409, Jun. 2018.
[40] J. Beil, C. Marquardt, and T. Asfour, "Self-aligning exoskeleton hip joint: Kinematic design with five revolute, three prismatic and one ball joint," in *Proc. Int. Conf. Rehabil. Robot. (ICORR)*, Jul. 2017, pp. 1349–1355.
[41] J. Wang *et al.*, "Comfort-centered design of a lightweight and backdrivable knee exoskeleton," *IEEE Robot. Autom. Lett.*, vol. 3, no. 4, pp. 4265–4272, Oct. 2018.
[42] B. Choi *et al.*, "A self-aligning knee joint for walking assistance devices," in *Proc. 38th Annu. Int. Conf. IEEE Eng. Med. Biol. Soc. (EMBC)*, Aug. 2016, pp. 2222–2227.
[43] Y. Niu, Z. Song, and J. Dai, "Kinematic analysis and optimization of a planar parallel compliant mechanism for self-alignment knee exoskeleton," *Mech. Sci.*, vol. 9, no. 2, pp. 405–416, Nov. 2018.
[44] Y. Niu, Z. Song, and J. S. Dai, "Design of the planar compliant five-bar mechanism for self-aligning knee exoskeleton," in *Proc. Int. Conf. Reconfigurable Mech. Robots (ReMAR)*, Jun. 2018, pp. 1–7.
[45] X. Tang and L. Chen, "Structural design of a novel wearable knee exoskeleton," in *Proc. ICMSE*, vol. 164, 2018, pp. 348–353.
[46] A. H. A. Stienen *et al.*, "Dampace: Design of an exoskeleton for force-coordination training in upper-extremity rehabilitation," *J. Med. Devices*, vol. 3, no. 3, pp. 031003-1–031003-10, Sep. 2009.
[47] M. A. Ergin and V. Patoglu, "ASSISTON-SE: A self-aligning shoulder-elbow exoskeleton," in *Proc. IEEE Int. Conf. Robot. Automat.*, May 2012, pp. 2479–2485.
[48] T. Lenzi *et al.*, "Measuring human–robot interaction on wearable robots: A distributed approach," *Mechatronics*, vol. 21, no. 6, pp. 1123–1131, Sep. 2011.
[49] K.-Y. Wu, Y.-Y. Su, Y.-L. Yu, C.-H. Lin, and C.-C. Lan, "A 5-degrees-of-freedom lightweight elbow-wrist exoskeleton for forearm fine-motion rehabilitation," *IEEE/ASME Trans. Mechatronics*, vol. 24, no. 6, pp. 2684–2695, Dec. 2019.